Synthesis and Thermal Properties of Phase-Change Microcapsules Incorporated with Nano Alumina Particles in the Shell

Ling Chen,[1] Li-Qun Zhang,[1,2,3] Rui-Fen Tang,[1] Yong-Lai Lu[1,2,3]

[1]*Key Laboratory of Beijing City on Preparation and Processing of Novel Polymer Materials*
[2]*Key Laboratory of Carbon Fiber and Functional Polymer, Chinese Ministry of Education; College of Material Science and Engineering, Beijing University of Chemical Technology, Beijing 100029, People's Republic of China*
[3]*State Key Laboratory of Organic-Inorganic Composites, Beijing University of Chemical Technology, Beijing 100029, People's Republic of China*

Received 21 February 2011; accepted 2 June 2011
DOI 10.1002/app.35027
Published online 10 October 2011 in Wiley Online Library (wileyonlinelibrary.com).

ABSTRACT: Novel phase-change microcapsules with paraffin as core and melamine-formaldehyde (MF) resin as shell were synthesized through *in situ* polymerization, in which nano alumina (nano-Al_2O_3) particles were dispersed in the shell by mixing nano-Al_2O_3 with MF prepolymer solution using the direct addition method (i.e., adding nano-Al_2O_3 into the MF prepolymer solution directly) and the predispersed addition method (i.e., predispersing the nano-Al_2O_3 homogenously in water under the assistance of dispersant and wetting agents before mixing with the MF prepolymer). Scanning electron microscope experiments demonstrated that the predispersed addition method yielded the microcapsules having the better dispersion and less self-agglomeration of alumina, compared to the direct addition method. Fourier transform infrared spectroscopy, energy dispersive X-ray spectroscopy, and electron backscatter diffraction imaging confirmed that the nano-Al_2O_3 particles were successfully incorporated in the shell by the predispersed addition method. The phase change behavior of microcapsules incorporated with different contents (up to 12.7% relative to the microcapsule) of nano-Al_2O_3 particles in the shell was investigated by differential scanning calorimeter. The results revealed that the encapsulation efficiency for this kind of novel microcapsules was >77% and the incorporation of nano-Al_2O_3 in the shell affected the phase change temperature. Thermal gravimetric analysis indicated that the addition of nano-Al_2O_3 improved the thermal stability of microcapsules remarkably. © 2011 Wiley Periodicals, Inc. J Appl Polym Sci 124: 689–698, 2012

Key words: microencapsulation; nanoparticle; thermal properties; phase-change materials; paraffin

INTRODUCTION

Phase-change microcapsules are granular substances with a core shell structure, where the phase-change materials form the core enwrapped by the shell material.[1] The microcapsules diameters are in the range of less than 1 μm to more than 1000 μm.[2] Microencapsulated phase change materials have been studied since the 1970s[3] and have attracted more and more attention in recent years. Various techniques have been used for preparation of phase-change microcapsules, including *in situ* polymerization,[4–7] interfacial polymerization,[8–10] emulsion polymerization,[11,12] complex coacervation,[13] and spray-drying methods.[14] Phase-change microcapsules have been applied in the fields of thermoregulated fibers,[6,15–18] heat energy transfers,[19–21] and energy-saving building materials.[22–24]

The shell materials have a great effect on properties of microcapsules, and the requirements varied with the applications. The choice of suitable shell materials plays an important role in the application. To provide good protection for the core, microcapsules have been synthesized with melamine formaldehyde (MF) resin,[4,5,21,22] urea-formaldehyde resin,[25–27] and polyurethane[28–30] as shell materials. However, the brittleness of these shell materials is still an obstacle to the industrial application of the microcapsules.[31] The studies on the modification of these microcapsules are seldom reported at present, and researches on the filling of shell materials with nano particles are especially rare. Song et al.[1] fabricated novel phase-change microcapsules that were filled with silver nano particles, with aminoplast as the wall and the phase change material bromo-hexadecane as the core, through *in situ* polymerization. Thermal gravimetric (TG) analysis confirmed that nanocomposite phase-change microcapsules had higher thermal stability than that of conventional phase-change microcapsules. They attributed this to nanocomposite structure of the microcapsules, in

Correspondence to: Y.-L. Lu (luyonglai@hotmail.com).

TABLE I
The Formula for Preparation of the Microcapsules Incorporated with Different Amount of Nano-Al_2O_3

Microcapsules		(a)	(b)	(c)	(d)	(e)	(f)
Core	Paraffin (g)				20		
	Emulsifier (g)				10		
	Distilled water (mL)				200		
Shell	Melamine (g)				3		
	Formaldehyde (mL)				10		
	Distilled water (mL)				20		
Filler	Nano-Al_2O_3 (g)	0	0.6	0.9	2.0	3.0	4.0
Content of nano-Al_2O_3 in the microcapsule (wt %)		0	2.2	3.3	6.8	9.8	12.7
Content of nano-Al_2O_3 in the shell (wt %)		0	7.7	11.1	21.1	28.6	34.8

which metal silver nanoparticles distributed on the surface to increase wall toughness and strength. However, the price of silver is relative high. We expected that using some inexpensive inorganic nanofillers might also improve the thermal stability of the phase-change microcapsules.

In this study, novel phase-change microcapsules incorporated with nano-Al_2O_3 particles in MF resin shell were synthesized through *in situ* polymerization by using paraffin (melting point 48–50°C) as core material. The aims of this work are to compare two different addition methods of nano-Al_2O_3 for the optimal microcapsule preparation procedure and to investigate the effects of nano-Al_2O_3 addition quantity on the microstructure, phase change behavior, and thermal properties of the resultant microcapsules.

EXPERIMENTAL

Materials

Melamine with purity >99.5% and formaldehyde (37 wt % aqueous solution) used as shell-forming monomers were purchased from Beijing Chemical Reagent Company, China. Paraffin used as core phase-change materials with a melting point of around 48–50°C was also obtained from Beijing Chemical Reagent Company, China. Sodium salt of styrene-maleic anhydride copolymer (SMA) used as emulsifier was kindly supplied by Shanghai Leather Chemical Company, China. Acetic acid and triethanolamine, used as pH controllers, were purchased from Beijing Fine Chemicals Company and Beijing Chemical Reagent Company, respectively. Nano-Al_2O_3 particles with a diameter of about 100 nm were purchased from Dalian Luming Nano Science and Technology, China. Dispersant DP-270 and wetting agent TRITON X-405 were purchased from Beijing Sinmaya Chemicals.

Synthesis of phase-change microcapsules

The synthesis of the microcapsuled paraffin with an alumina nano particles-filled MF resin shell was carried out in a 500-mL three-neck round-bottomed flask equipped with a condenser and a poltytetrafluoroethylene mechanical stirrer, as following procedures.

First, 20.0 g of solid paraffin and 10.0 g of sodium salt of SMA copolymer were dissolved in 200 mL of distilled water at 80°C. When the solid paraffin melted, the mixture was emulsified mechanically under a vigorous stirring rate of 900 rpm for 2 h by using a JHS-1/90 high-speed disperse machine (Hangzhou Instrument Electric, Hangzhou, China). Then the pH value of the oil-in-water emulsion was adjusted to 4–5 with 15 wt % acetic acid solution.

Second, the aqueous solution of MF prepolymer was prepared by mixing 3.0 g of melamine, 10.0 mL of formaldehyde, and 20.0 mL of distilled water in a 100 mL three-neck round-bottomed flask at 70°C under a stirring rate of 300 rpm. The pH value of the prepolymer solution was adjusted to 8.5–9.0 with 10 wt % triethanolamine. After 30 min, the solution became transparent, and a certain amount of nano-Al_2O_3 powder (Table I for detailed process parameters) was added to the prepolymer solution. Two different methods were applied to disperse the nano-Al_2O_3 particles in the prepolymer solution. One is the direct addition method: the dried alumina powder was mixed into the prepolymer solution directly. The other is predispersed addition method: 10 g of alumina powder was added in 100 mL of distilled water containing 1 mL of dispersant and 0.5 mL of wetting agent, followed by high-speed stirring at 9600 rpm for 30 min. The obtained alumina aqueous suspension was added into the prepolymer solution, and then the mixture was continuously stirred for 10 min.

Third, the stirring rate of the emulsion was adjusted to 300 rpm, and the prepolymer solution containing nano-Al_2O_3 particles was added drop wise to the emulsion at a dropping speed of about 1.5 mL/min to start *in situ* polymerization. After all of the prepolymer was added, the stirring continued for 2 h. The pH of the emulsion was adjusted to 9.0 with 10 wt % triethanolamine solution, which terminated the reaction. Then the resultant microcapsules were filtered out and washed with distilled water at approximately 70°C until a pH of 7 was reached.

The wet microcapsule powders were dried in a vacuum oven at 40°C for 24 h to remove the water.

Characterization

Chemical characterization

Fourier transform infrared spectroscopy (FTIR) spectra of solid paraffin, alumina powder, and the microcapsules were obtained by using a Bruker Tensor-27 FTIR spectrophotometer at a scanning number of 32 and wave numbers range of 4000–400 cm^{-1}.

Surface morphology

The morphology of the dried microcapsules was observed by using scanning electron microscope (SEM, Hitachi *S*-4700, Japan) under a performing voltage of 3 kV.

Surface elemental analysis

An energy dispersion X-ray microanalyzer was used, which was attached to the SEM system, to examine the elemental compositions of the microcapsules. The basic principal of energy dispersive X-ray spectroscopy (EDX) is defined as a microanalytical technique that uses the characteristic energy spectrum of X-rays emitted by the specimen after excitation by high-energy electrons to obtain information about the elemental composition, as described in the Ref. [1] The data treatment software used a φ-ρ-Z approach to determine the element contents as atom percentage and mass percentage.[32]

DSC and thermal gravimetry (TG) analyses

The phase change properties of the dried microcapsules and core material paraffin were measured by using a differential scanning calorimeter (DSC, DSC-STA Re, METTLER-TOLEDO) at heating and cooling rates of 10°C/min in a nitrogen atmosphere. For each sample, the temperature ranges of the heating and cooling cycles were 0 to 80°C and 80 to 0°C, respectively. The weight of each sample was about 6 ± 1mg.

The percentage of paraffin is a key parameter for the microcapsules.[12] It determines directly the enthalpy, and thus the energy storage efficiency of the microcapsules. The specific heat of paraffin is a constant in the measured temperature range,[33] and there is no phase transition of MF resin (i.e., the wall material) in this temperature range. Therefore, the content of paraffin in the microcapsules can be estimated according to the following equation:

$$\text{Paraffin content}(\%) = \left(\frac{\Delta H_{\text{m,microcapsules}} + \Delta H_{\text{c,microcapsules}}}{\Delta H_{\text{m,paraffin}} + \Delta H_{\text{c,paraffin}}}\right) \times 100 \quad (1)$$

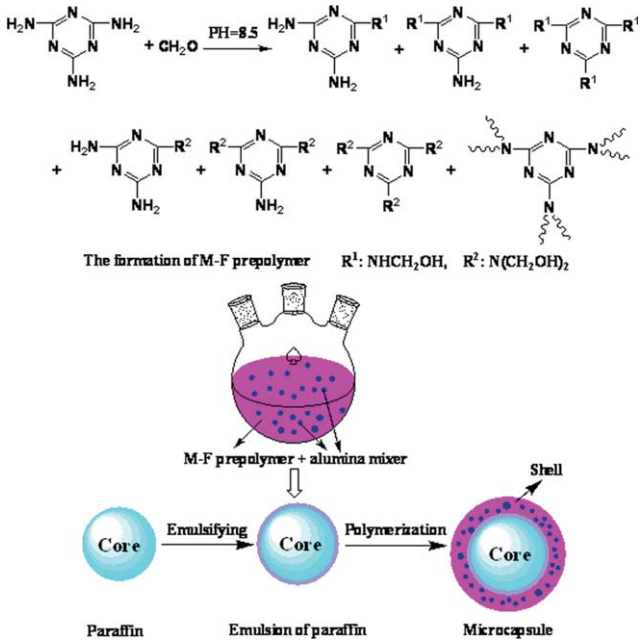

Figure 1 Schematic diagram depicting the formation of the microcapsules filled with nano alumina particles in the shell. [Color figure can be viewed in the online issue, which is available at wileyonlinelibrary.com]

where $\Delta H_{\text{m, microcapsule}}$ and $\Delta H_{\text{c, microcapsule}}$ are the latent heat of melting and the heat of crystallization of the microcapsules, respectively, and $\Delta H_{\text{m, paraffin}}$ and $\Delta H_{\text{c, paraffin}}$ are the latent heat of melting and the heat of crystallization of the phase-change paraffin, respectively.

The thermal stability of the samples was characterized by measuring the weight loses with temperature increasing from 30 to 800°C in nitrogen gas flow using a thermogravimetric analyzer (TGA, TGA-STA Re, METTLER-TOLEDO) at a scanning rate of 20°C/min.

RESULTS AND DISCUSSION

Fabrication of microcapsules

The formation of microcapsules filled with nano-Al_2O_3 particles is presented schematically in Figure 1. According to previous literatures[2,4,8,33] about preparation of the phase-change microcapsule with *in situ* polymerization method, we brought out the formation mechanism of the phase-change microcapsule incorporated with nano-Al_2O_3 particles in the shell. First, the core material, paraffin, was emulsified under the condition of high temperature and high stirring rate with SMA as the emulsifier. During this process, the hydrophilic aryl groups of emulsifer insert into the core paraffin, and hydrophobic anionic —COO groups directionally arrange out of the core paraffin. As a result, the surface of

core droplets became negatively charged. Second, the aqueous solution of the MF prepolymer containing nano-Al_2O_3 was added drop wise into acidic paraffin emulsion. Under acidic condition, the MF prepolymer obtained H^+ changing into positively charged active prepolymer. Negatively charged paraffin droplets had affinity for modified MF prepolymer by static, so the modified MF prepolymer was adsorbed to the surface of the paraffin emulsion. Because the environmental condition of MF prepolymer changed from originally alkaline to acidic, the further polymerization of MF prepolymers was initialized, and as a result, the crosslinking degree of the MF prepolymer increased gradually and its solubility in water decreased. Finally, The MF resin precipitated from the aqueous phase and formed a compact shell enclosing the core material finally. The nano-Al_2O_3 is hydrophilic, and the predispersing process further increased the hydrophilicity of nano-Al_2O_3. On the contrary, the core material (i.e., paraffin) is hydrophobic. Therefore, during the formation of the shell, the nano-Al_2O_3 particles would prefer to disperse in the MF prepolymer aqueous solution rather than enter into core materials. Moreover, the paraffin core material was emulsified before adding MF prepolymer containing nano-Al_2O_3, and therefore, the static resistance of the emulsifier would also prevent the nano particles from entering into core materials. Consequently, the phase-change microcapsules incorporated with nano alumina particles in the shell can be prepared by proposed approach in this study.

FTIR spectra

Figure 2 shows the FTIR spectra of nano-Al_2O_3, pure paraffin, and microcapsules with or without nano-Al_2O_3 particles in the shell. The broad absorption peaks at approximately 3418 cm^{-1} are associated with the O—H stretching vibration and N—H stretching vibration for some samples [i.e., spectra (a), (b), and (c)]. The peaks at 2957, 2918, and 2850 cm^{-1} arise from the C—H stretching vibration modes. The peak associated with the C—N multiple stretching vibration in the triazine ring is found at 1559 cm^{-1}, and the characteristic bending vibration peak for the triazine ring is found at 814 cm^{-1}.[2] Meanwhile, the C—O—C stretching vibration peaks at 1009 and 1163 cm^{-1} can be observed, which are the specific absorption bands of MF resin and confirms the existence of the MF shell of the microcapsules. In addition, the FTIR spectra of these microcapsules (i.e., a-c) also show the characteristic absorption bands of paraffin in Figure 2(d) at 1464, 1360, and 720 cm^{-1}, corresponding to the C-H bending vibrations and the in-plane rocking vibration of the methylene group, thus confirming the presence of paraffin in the resultant microcapsules. The FTIR spectra of the alumina is presented in Figure 2(e), in which the characteristic absorption peaks responsible for Al—O vibrations are observed around 597 and 451 cm^{-1}.[34] In the spectra of the microcapsules whose shells were incorporated with nano-Al_2O_3 particles [Fig. 2(a,b)], the specific absorption peaks of alumina can be observed, whereas none of these specific peaks appear in the spectrum of the microcapsule whose shell does not contain alumina [Fig. 2(c)]. These results confirm that nano-Al_2O_3 particles were successfully dispersed in the microcapsules prepared through whether the direct addition method or the predispersed addition method.

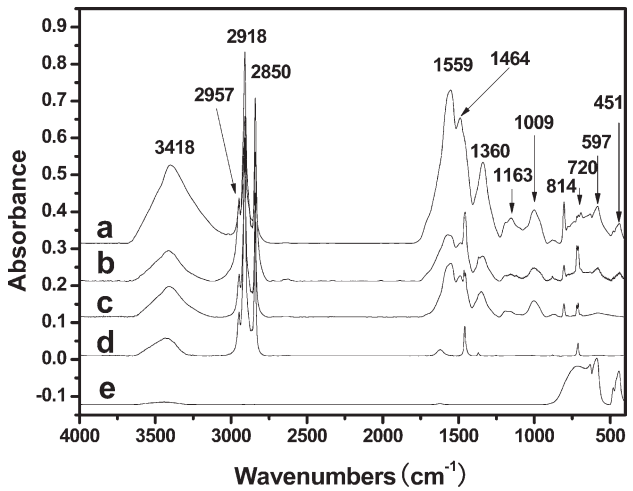

Figure 2 FTIR spectra of (a) Microcapsules filled with alumina in the shell by direct addition method, (b) microcapsules filled with alumina in the shell by predispersed addition method, (c) microcapsules without alumina in the shell, (d) pure paraffin, and (e) pure nano alumina.

Surface morphology

Influence of addition method of nano alumina on morphology of microcapsules

The SEM photographs of the microcapsules with alumina-filled shell prepared by different alumina addition methods are presented in Figure 3. Mass contents of alumina in both microcapsules are all 2.2%. It can be seen that most microcapsules synthesized through the direct addition method [Fig. 3(a)] are not spherical, and have a rough surface even for a few spherical microcapsules. Compared with the microcapsules synthesized by the direct addition method, the microcapsules prepared by the predispersed addition method [Fig. 3(b)] are all global and have relative smooth surface. Its particle size distribution is within the range from $\sim$ 70 to 110 μm.

The alumina particles used in this study are nanometer sized. It is known that nano alumina is prone to secondary agglomeration. Without adding any dispersant or wetting agent, the suspension of alumina particles depends mainly on electrostatic

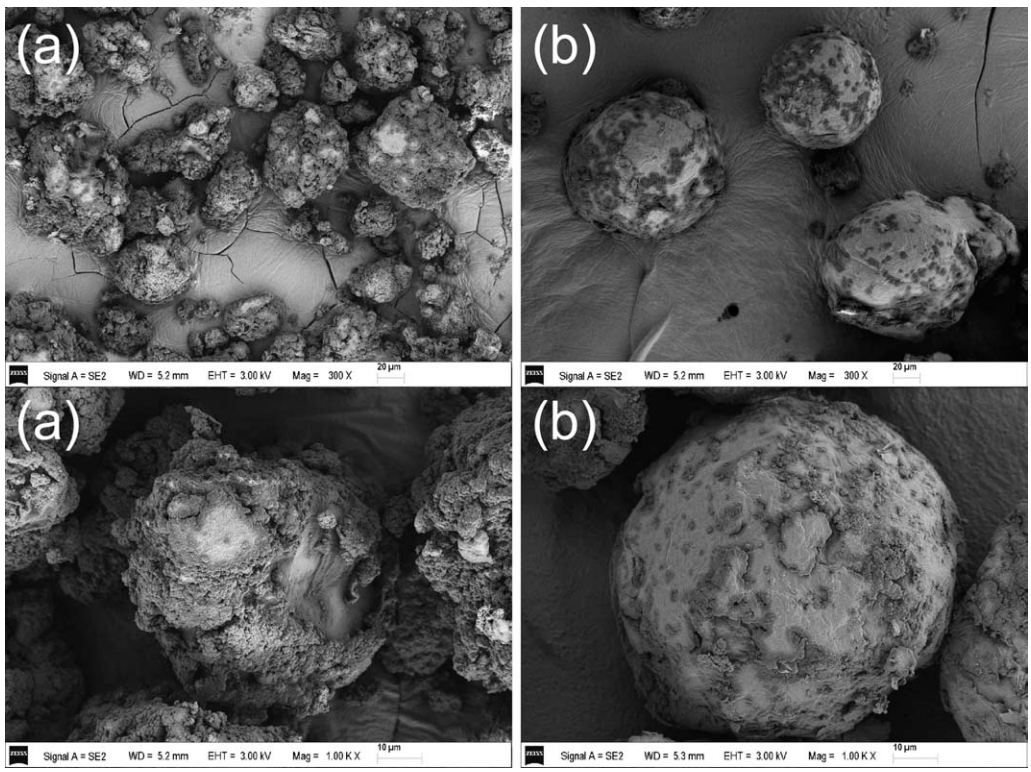

Figure 3 SEM photographs of the microcapsules with alumina in the shell prepared by different alumina addition methods: (a) direct addition method; (b) predispersed addition method.

repulsion and the buoyancy of water. Under the influence of gravity, the alumina particles tend to coagulate in MF prepolymer solution along with irregular Brownian motion. These uneven nano-Al_2O_3 agglomerates covered on the surface of microcapsules, resulting in a coarse and nonspherical surface. The dispersant and wetting agent can improve the dispersing ability of alumina in MF prepolymer solution and then overcome the effects of coagulation, and sedimentation. The dispersant DP 270 is a neutral low-molecular weight polyacrylic ester containing two parts in its molecular structure.[35] One part is the anchoring group (carboxyl group), which can be tightly absorbed on the surface of alumina particles through chemical bonding or hydrogen bonding, forming a negatively charged absorption layer. Another part is the water-soluble chain, which can be stretched in the water, forming a protective layer with adequate thickness. The modified alumina particles mutually repel each other because of the steric hindrance effect. A stable suspension of alumina particles in water is maintained under the dual effects of steric hindrance and electrostatic repulsion. The wetting agent TRITON X-405 is an alkyl phenol polyoxyethylene ether nonionic surfactant that can accelerate the wetting process of the alumina surface and improve the dispersion efficiency, enhancing the stability of the alumina suspension.

Influence of added amounts of alumina on morphology of microcapsules

Figure 4 presents the SEM photographs of the microcapsules containing different amounts of alumina in the shell prepared by the predispersed addition method. Figure 4(a) also shows the conventional microcapsules using paraffin as core material and MF resin without alumina filler as shell for comparison. The dispersion of the spherical microcapsules is relatively homogeneous without significant agglomeration. The surface of the microcapsules is relatively smooth and compact without any disfigurement of the shell, and the average size is about 80 μm. However, the high-magnification photo reveals that some nanoparticle-like raises exist on the surface of microcapsules. These nanoparticles are resulted from MF resin aggregate,[2] and commonly existed on the surface of phase change microcapsules having MF resin shell.[4,15,16,22,36,37] As shown in Figure 4(b–f), the microcapsules filled with 7.7%, 11.1%, 21.1%, 28.6%, and 34.8% nano-Al_2O_3 in the shell are also spherical. There is no obvious difference among microcapsules (a), (b), and (c) in shape and size distribution, indicating that the addition of a small amount of alumina particles has no negative effect on the formation of microcapsules. Furthermore, Figure 4 indicates that the surface roughness of the microcapsules increases with increasing amount of alumina in the shell. It can be been that the surfaces of

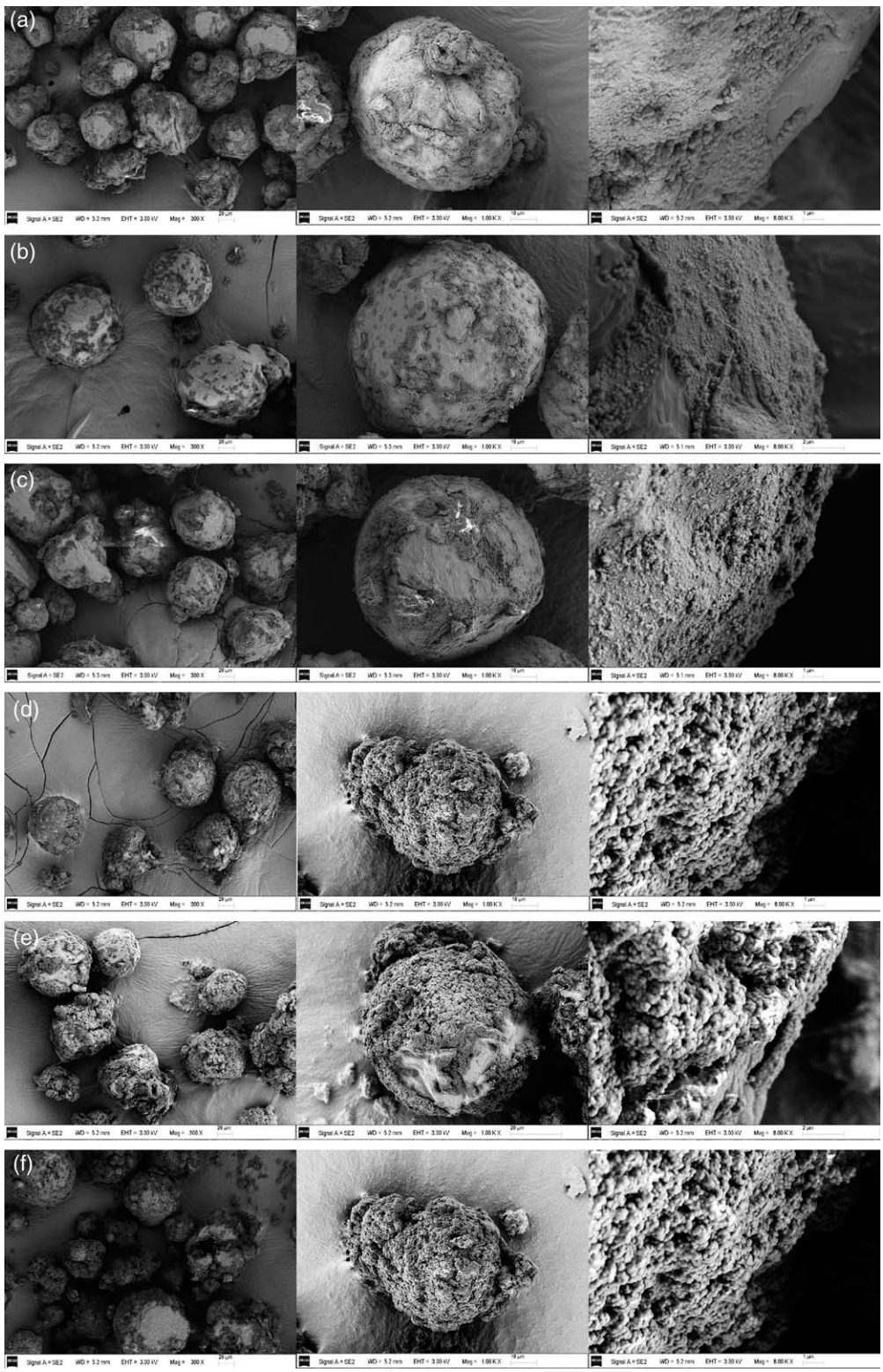

Figure 4 SEM photographs of the microcapsules containing different amounts of nano alumina in the shell: (a) 0%, (b) 7.7%, (c) 11.1%, (d) 21.1%, (e) 28.6%, and (f) 34.8%.

microcapsules (d), (e), and (f) are obviously rougher than those for microcapsules (a), (b), and (c). When alumina was added in the shell of microcapsules, the raises are MF resin nanoparticles and nano-Al_2O_3 nanoparticles covered by MF resin. With the increase of addition amount, the alumina agglomerate increase, leading to the size of alumina covered by MF resin becoming larger. Some broken microcapsules can be seen in Figure 4(f) for 34.8% alumina relative to the shell, indicating that excessive

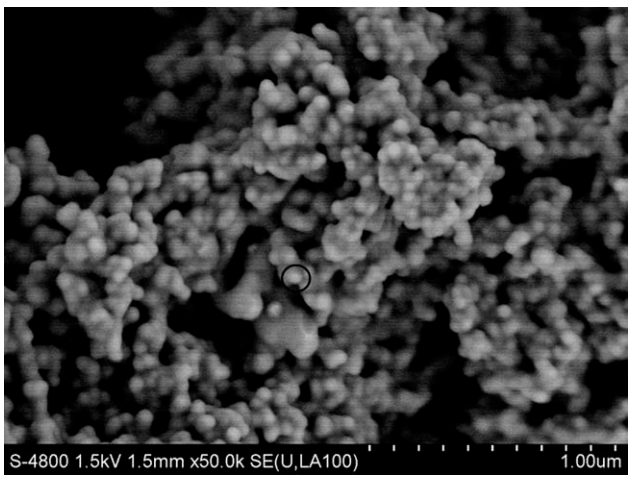

Figure 5 EBSD image of the microcapsule with 34.8% alumina in the shell.

alumina have negative influence on the adsorption of shell material on the surface of core. A possible explanation is that extensive agglomeration of alumina particles occurs in the MF resin shell when the amount of alumina reaches a critical value, leading to a nonuniform distribution of alumina in the shell and poor interface adhesion.

To determine the composition of these raised particles and the distribution state of nano alumina in the shell, we obtained electron backscatter diffraction (EBSD) image of the microcapsule with 34.8% alumina in the shell, as shown in Figure 5. EBSD is based on the acquisition of diffraction patterns from bulk samples in the SEM. The backscattered electron signal increases with the atomic number of the substance.[38] The EBSD image of the microcapsule surface shows that there are many bright spot-like regions (One of them was marked by black circle in the image as a sample) in contrast to the matrix, corresponding to a high atomic number region.[39] The diameter of these bright spot-like regions is about 100 nm, consisting with that of nano-Al_2O_3 used in this study. Therefore, the bright spot-like regions in the EBSD image represent nano-Al_2O_3 incorporated in the shell of the microcapsule.

Surface elemental analysis

EDX was used to study the surface elemental composition of the microcapsules. Figure 6 shows the

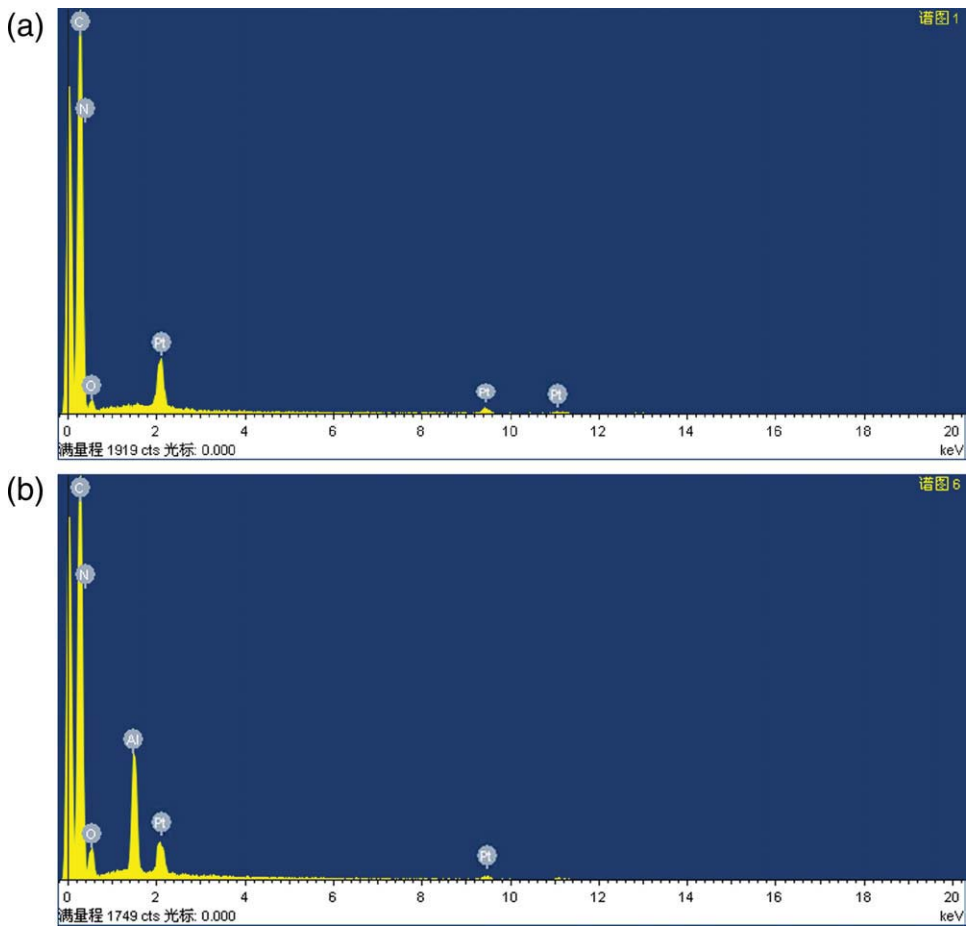

Figure 6 EDX spectra of the microcapsules: (a) without nano-Al_2O_3 and (b) incorporated 34.8% alumina in the shell. [Color figure can be viewed in the online issue, which is available at wileyonlinelibrary.com]

TABLE II
Experimental Data of EDX Analysis

Microcapsules	(a)	(b)	(c)	(d)	(e)	(f)
Weight content of element Al (wt %)	0	0.05	0.8	2.88	3.32	4.09
Atomic content of element Al (atm %)	0	0.02	0.38	1.37	1.58	1.94

EDX curves of the microcapsules (a) and (f). Table II presents the elemental content of Al in microcapsules a-f. The elements C, N, and O, which are the component elements of paraffin and MF resin, all appear in the spectrum of microcapsule a, while the element Al is detected, in addition to C, N, and O, on the surface of microcapsules b-f. These EDX results, together with the results of FTIR, SEM, and EBSD, confirm the existence of alumina particles on the surface of microcapsules b-f. Meanwhile, Table II shows that the content of Al increases from 0.02% in microcapsule b to 1.94% in microcapsule f with increasing nano-Al_2O_3 dosage.

Phase change behavior

The DSC thermograms of the microcapsules with different amounts of alumina in the shell are displayed in Figure 7, and the specific data of phase change behavior are presented in Table III. Figure 7(a) shows that all the heating curves have about the same shape with two peaks, implying that the paraffin used in this work may be a compound of two linear-chain alkanes with different numbers of carbon atoms. Table III shows that the melting temperatures of the paraffin are 33°C and 53.8°C, whereas the melting temperatures of microcapsule (a) without alumina in the shell are 33.6°C and 54.1°C, slightly higher than those of pure paraffin. The heat resistance of the MF resin shell leads to the lag in phase change. The melting temperatures of microcapsules (b)-(f) are 36°C–40°C and 54°C–62°C, higher than those of microcapsule (a), indicating that the addition of alumina to the microcapsule shell provides extra protection to the core material paraffin.[1] With increasing alumina content, the crystallization temperatures of microcapsules (b)-(f) increase initially and then decrease, probably because the small amount of alumina in the shell of the microcapsules might mainly play the role of nucleating agent during crystallization, while excess nano-Al_2O_3 existing in the core-shell interface might interfere with the crystallizing of core materials.

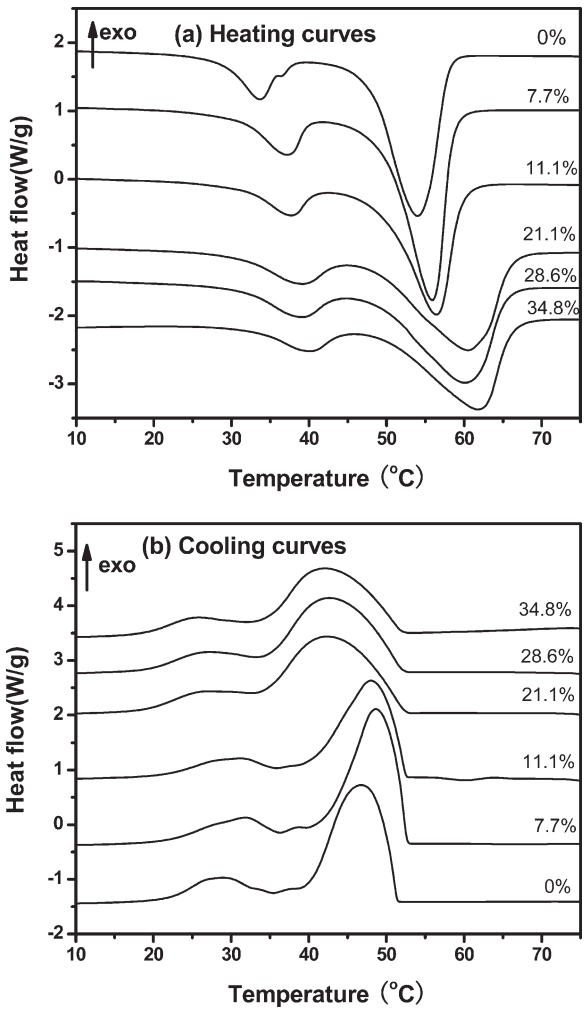

Figure 7 DSC curves of the microcapsules containing different amounts of alumina in the shell: (a) heating curves, and (b) cooling curves.

TABLE III
Phase-Change Properties of Pure Paraffin and the Microcapsules Containing Different Amounts of Alumina in the Shell

Samples	T_m (°C)		ΔH_m (J/g)	T_c (°C)		ΔH_c (J/g)	Average enthalpies (J/g)
Paraffin	33.0	53.8	168.1	49.0	29.0	164.5	166.3
(a)	33.6	54.1	112.7	47.3	28.7	106.5	109.6
(b)	36.9	55.5	115.3	49.1	31.8	110.6	113.0
(c)	37.4	56.1	98.3	48.4	31.9	87.9	98.1
(d)	38.7	60.2	101.4	43.1	26.1	89.4	95.4
(e)	38.6	59.9	94.4	43.2	26.2	88.5	91.4
(f)	39.8	61.6	84.1	42.6	25.2	79.1	81.6

TABLE IV
Theoretical and Experimental Contents of Paraffin in Microcapsules

Microcapsules	(a)	(b)	(c)	(d)	(e)	(f)
Ideal paraffin content/%	72.6	71.2	70.4	67.8	65.6	63.5
Experimental paraffin content/%	65.9	68.0	59.0	57.4	55.0	49.1
Encapsulation efficiency	0.91	0.96	0.84	0.85	0.84	0.77

Similarly, Wang et al. also[40–42] reported that the core-shell interface could obviously affect the crystallization behavior and structure of the *n*-alkane encapsulated in the microcapsule.

Table III also summarizes the phase change enthalpy of paraffin and the microcapsules. Microcapsule (a) has a phase change enthalpy of 110 J/g, lower than the value of 166 J/g for paraffin because the shell did not undergo phase changing within the experimental temperature range. As a result, the percentage of paraffin in the microcapsules can be estimated according to the measured enthalpy by using eq. (1).[2,12,33] The ideal paraffin content in the microcapsules is calculated according the actual dosage of paraffin, MF resin, and nano-Al_2O_3. The amounts of paraffin and MF resin used were fixed in the synthesis of microcapsules. The ideal content of the paraffin should decrease with increasing of nano alumina dosage. Here, the encapsulation efficiency was defined to represent how much fed paraffin had been encapsulated in the shell, which can be derived from following equation:

$$\text{Encapsulation efficiency}(\%) = \frac{\text{Experimental paraffin content}}{\text{Ideal paraffin content}} \times 100 \quad (2)$$

Table IV summarizes the experimental and ideal paraffin contents and encapsulation efficiencies for the microcapsules incorporated different amounts of nano-Al_2O_3 in the shell. The results reveal that hat the encapsulation efficiency is >0.77 for all microcapsules, and microcapsule (b) has the highest encapsulation efficiency of 0.96, indicating that majority of paraffin had be encapsulated in the shell through our processing procedure. It can be also found that, with increasing alumina content, the encapsulation efficiency increases initially and then decreases, implying that the insulating effect of the shell is improved with addition of a small amount of alumina, but further addition would result in negative effect on the encapsulation efficiency. A possible explanation is that the large surface areas of nano-Al_2O_3 particles enable them to be closely combined with the MF resin to form a composite shell that has high strength to resist crack,[1] on the condition that the amount of alumina added is not excessive. Excessive amounts of alumina can lead to agglomeration of particles, resulting in an uneven distribution of alumina particles in the shell and poor adhesion with the shell.[35] As a result, some formed shell might have loose and porous structures, so that the core material could leak out easily,[2] reducing the paraffin content in the resultant microcapsule. Obviously, the more dosage of nano-Al_2O_3, the more agglomerates of alumina. The lowest encapsulation efficiency of microcapsule (f) is probably due to the leakage of paraffin from broken microcapsules, which have been observed in Figure 4(f). These results also suggest that excessive alumina should have negative effect on the adsorption of shell material on the surface of core. Accordingly, the maximum dosage of nano-Al_2O_3 can reach 12.7% in the whole microcapsule or 34.8% in the shell.

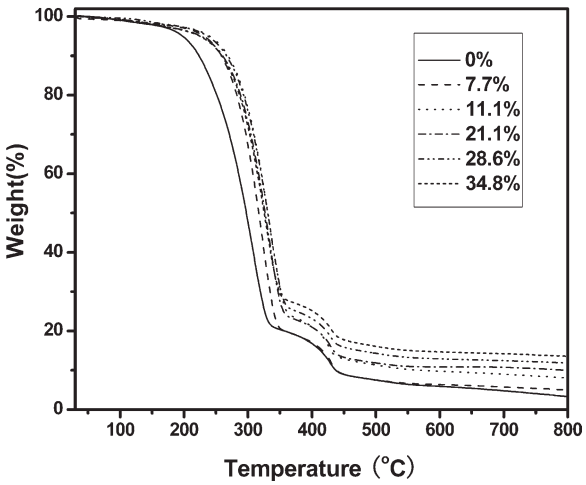

Figure 8 TG curves of the microcapsules containing different amounts of alumina in the shell.

Thermal stability

Figure 8 shows the TG thermograms of the microcapsules with different amounts of alumina in the shell, and the TG data are also summarized in Table V. It is observed that the weight loss profiles of all the microcapsules are quite similar, and weight loss occurs through two-step degradation. The first stage

TABLE V
Thermal Properties of the Microcapsules Containing Different Amounts of Alumina in the Shell

Microcapsules	(a)	(b)	(c)	(d)	(e)	(f)
Theoretical alumina content in the shell (%)	0	7.7	11.1	21.1	28.6	34.8
Weight loss temperature for peak 1 (°C)	308	322	335	328	330	323
Weight loss temperature for peak 2 (°C)	428	430	425	424	423	425

of the weight loss is attributed to the evaporation of paraffin. A sharp weight loss occurs at around 308°C for microcapsule (a) without alumina in the shell, and about 322–335°C for microcapsules (b)-(f). The increase in decomposition temperature of about 20°C indicates that the addition of alumina in the shell can improve the thermal stability of the microcapsules significantly. This increase can be attributed to the increased wall toughness and strength[1] as a result of the reinforcing effect of nano alumina. The second stage of the weight loss for all of the microcapsules occurs in the temperature range 423–430°C, corresponding to the degradation of the shell materials.

CONCLUSIONS

a. Phase-change microcapsules with paraffin (melting point around 48–50°C) as the core and MF resin as the shell were synthesized by *in situ* polymerization. The nano-Al_2O_3 particles were successfully incorporated in the wall of the microcapsules by mixing alumina with the MF prepolymer solution through the predispersed addition method, which were confirmed by FTIR, EDX, and EBSD experiments. SEM showed that the surface roughness of the microcapsules increased with increasing amount of alumina added.
b. DSC results showed that the incorporation of alumina to the shell affected the phase-change temperature of the microcapsules. With increasing alumina content, the melting temperature increased and the crystallization temperature first increased and then decreased. Besides, DSC results demonstrated that the encapsulation efficiency was >77% for all microcapsules. In combination with SEM analysis, the DSC results suggested that the maximum addition quantity of nano-Al_2O_3 in the microcapsules might be 12.7% (34.8% of the shell).
c. TG analysis revealed that the microcapsules with nano-Al_2O_3 in the shell have higher thermal stability than those without nano-Al_2O_3. The decomposition temperature increased by an average of 20°C with the addition of nano-Al_2O_3.

The authors thank the National Nature Science Foundation of China (Grant No. 50873007), Beijing Nature Science Foundation (2082019), Program for Changjiang Scholars and Innovative Research Team in University (PCSIRT, IRT0807) and Beijing Nova Program of Science and Technology (2006A15) for their financial supports.

References

1. Song, Q. W.; Li, Y.; Xing, J. W.; Hu, J. Y.; Marcus, Y. Polymer 2007, 48, 3317.
2. Zhang, H. Z.; Wang, X. D. Colloid Surface A 2009, 332, 129.
3. Zhang, X. X.; Fan, Y. F.; Tao, X. M.; Yick, K. L. Mater Chem Phys 2004, 88, 300.
4. Su, J F.; Wang, L. X.; Ren, L. J Appl Polym Sci 2006, 101, 1522.
5. Shin, Y.; Yoo, D. I.; Son, K. J Appl Polym Sci 2005, 96, 2005.
6. Sarier, N.; Onder, E. Thermochim Acta 2007, 452, 149.
7. Zhang, X. X.; Fan, Y. F.; Tao, X. M.; Yick, K. L. J Colloid Interface Sci 2005, 281, 299.
8. Su, J. F.; Wang, L. X.; Ren, L. Colloid Surface A 2007, 299, 268.
9. Zhang, H. Z.; Wang, X. D. Sol Energy Mater Sol Cells 2009, 93, 1366.
10. Sullivan, M.; Vincent, B. J Colloid Interface Sci 2010, 343, 31.
11. Alkan, C.; Sarı, A.; Karaipekli, A.; Uzun, O. Sol Energy Mater Sol Cells 2009, 93, 14.
12. Sar, A.; Alkan, C.; Karaipekli, A. Appl Energ 2010, 87, 1529.
13. Hawladera, M. N. A.; Uddina, M. S.; Khin, M. M. Appl Energ 2003, 74, 195.
14. Petrovic, L. B.; Sovilj, V. J.; Katona, J M; Milanovic, J L J Colloid Interface Sci 2010, 342, 333.
15. Fan, Y. F.; Zhang, X. X.; Wu, S. Z.; Wang, X. C. Thermochim Acta 2005, 429, 25.
16. Hong, K.; Park, S. Mater Chem Phys 1999, 58, 128.
17. Xing, JW.; Li, Y.; Newton, E. US, Pat, 74424107442410; 2008.
18. Sánchez, P.; Fernandez, M. V. S.; Romero, A.; Rodríguez, J. F.; Silva, L. S. Thermochim Acta 2010, 498, 16.
19. Li, J L.; Xue, P.; Ding, W. Y.; Han, J. M.; Sun, G. L. Sol Energy Mater Sol Cells 2009, 93, 1761.
20. Hawlader, M. N. A.; Uddin, M. S.; Zhu, H. J. Int J Energy Res 2002, 26, 159.
21. Su, J F.; Wang, L. X.; Ren, L.; Huang, Z. J Appl Polym Sci 2007, 103, 1295.
22. Su, J F.; Wang, L. X.; Ren, L. J Appl Polym Sci 2005, 97, 1755.
23. Zhang, Y. P.; Lin, K. P.; Yang, R.; Di, H. F.; Jiang, Y. Energ Bldg 2006, 38, 126.
24. Hunger, M.; Entrop, A. G.; Mandilaras, I.; Brouwers, H. J. H.; Founti, M. Cem Concr Compos 2009, 31, 731.
25. Gao, G. B.; Qian, C. X.; Gao, M. J Chin Chem L 2010, 21, 533.
26. Park, S. J; Shin, Y. S.; Lee, J. R. J Colloid Interface Sci 2001, 241, 502.
27. Guo, H. L.; Zhao, X. P.; Wang, J. P. J Colloid Interface Sci 2005, 284, 646.
28. You, M.; Zhang, X. X.; Wang, X. C.; Zhang, L.; Wen, W. Thermochim Acta 2010, 500, 69.
29. Cho, J S.; Kwon, A.; Cho, C. G. Colloid Polym Sci 2002, 280, 260.
30. Rodríguez, S. N.; Fernandes, I.; Martins, I. M.; Mata, V. G.; Barreiro, F.; Rodrigues, A. E. Ind Eng Chem Res 2008, 47, 4142.
31. Gong, C. Y.; Zhang, H. Z.; Wang, X. D. Iran Polym J 2009, 6, 501.
32. Jeffrey, R. S. B.; Cecile, G., Claude, L. C. Chem Mater 2006, 18, 6397.
33. Li, W.; Zhang, X. X.; Wang, X. C.; Niu, J. J Mater Chem Phys 2007, 106, 437.
34. Saravanan, L.; Subramanian, S. J Colloid Interface Sci 2005, 284, 363.
35. Wang, Z. D.; Hu, L. M. Speciality Chemicals 1996, 11, 59.
36. Salaün, F.; Devaux, E.; Bourbigot, S.; Rumeau, P.; Chapuis, P. O.; Saha, S. K.; Volz, S. Thermochim Acta 2008, 477, 25.
37. Fan, Y. F.; Zhang, X. X.; Wang, X. C.; Li, J.; Zhu, Q. B. Thermochim Acta 2004, 413, 1.
38. Humphreys, F. J. Scripta Mater 2004, 51, 771.
39. Liu, L. L.; Sun, W.; Wang, F.; Zhang, Z. J Chinese Electron Microsc Soc 2008, 27, 266.
40. Xie, B.; Shi, H.; Jiang, S.; Zhao, Y.; Han, C. C.; Xu, D.; Wang, D. J. J Phys Chem B 2006, 110, 14279.
41. Xie, B.; Liu, G.; Jiang, S.; Zhao, Y.; Wang, D. J. J Phys Chem B 2008, 112, 13310.
42. Jiang, K.; Su, Y.; Xie, B.; Jiang, S.; Zhao, Y.; Wang, D. J.f J Phys Chem B 2008, 112, 16485.